

UQGAN: A Unified Model for Uncertainty Quantification of Deep Classifiers trained via Conditional GANs

Philipp Oberdiek¹, Gernot A. Fink¹, and Matthias Rottmann²

¹Department of Computer Science, TU Dortmund University

²School of Mathematics and Natural Sciences, University of Wuppertal

Abstract

We present an approach to quantifying both aleatoric and epistemic uncertainty for deep neural networks in image classification, based on generative adversarial networks (GANs). While most works in the literature that use GANs to generate out-of-distribution (OoD) examples only focus on the evaluation of OoD detection, we present a GAN based approach to learn a classifier that exhibits proper uncertainties for OoD examples as well as for false positives (FPs). Instead of shielding the entire in-distribution data with GAN generated OoD examples which is state-of-the-art, we shield each class separately with out-of-class examples generated by a conditional GAN and complement this with a one-vs-all image classifier. In our experiments, in particular on CIFAR10, we improve over the OoD detection and FP detection performance of state-of-the-art GAN-training based classifiers. Furthermore, we also find that the generated GAN examples do not significantly affect the calibration error of our classifier and result in a significant gain in model accuracy.

1 Introduction

Deep learning has shown outstanding performance in image classification tasks [He et al. \[2016\]](#), [Krizhevsky et al. \[2012\]](#), [Simonyan and Zisserman \[2015\]](#). However, due to the enormous capacity and the inability of rejecting examples, deep neural networks (DNNs) are not capable of expressing their uncertainties appropriately. DNNs have demonstrated the tendency to overfit training data [Srivastava et al. \[2014\]](#) and to be easily fooled into wrong class predictions with high confidence [Goodfellow et al. \[2015\]](#), [Guo et al. \[2017\]](#). Also, importantly, ReLU networks have been proven to show high confidence far away from training data [Hein et al. \[2019\]](#). This is contrary to the behavior that would be expected naturally by humans, which is to be uncertain when being confronted with new data examples that have not been observed during training.

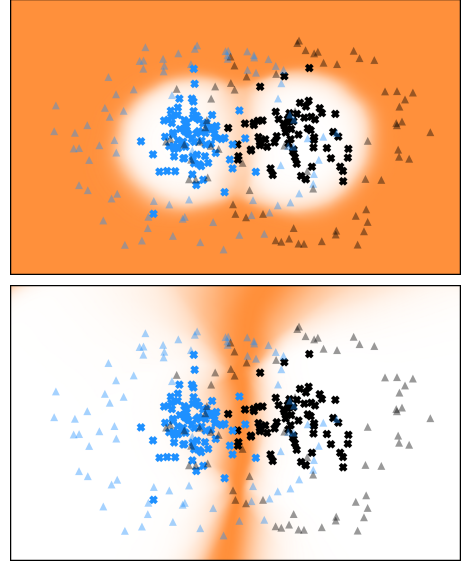


Figure 1: Toy example of two slightly overlapping Gaussian distributions. From top to bottom: 1. OoD heatmap with orange indicating a high probability of being OoD and white of in-distribution; 2. Aleatoric uncertainty (entropy over Equation (1)) with orange indicating high and white low uncertainty. Triangles indicate GAN-generated out-of-class examples and crosses correspond to the in-distribution data, while their color is coding the class membership.

Several approaches to predictive uncertainty quantification have been introduced in recent years, considering uncertainty in a Bayesian sense [Blundell et al. \[2015\]](#), [Gal and Ghahramani \[2015\]](#), [Kendall and Gal \[2017\]](#) as well as from a frequentist’s point of view [DeVries and Taylor \[2018\]](#), [Hendrycks and Gimpel \[2017\]](#), [Padhy et al. \[2020\]](#). A common evaluation protocol is to discriminate between true and false positives (FPs) by means of a given uncertainty quantification. For an introduction to uncertainty in machine learning, we refer to [Hüllermeier and Waegeman \[2021\]](#), for a survey on uncertainty quantification methods for DNNs see

Gawlikowski et al. [2021].

By design of ordinary DNNs for image classification, their uncertainty is often studied on in-distribution examples Ashukha et al. [2020]. The task of out-of-distribution (OoD) detection (or novelty detection) is oftentimes considered separately from uncertainty quantification Liang et al. [2018], Mundt et al. [2019], Snoek et al. [2019]. Thus, OoD detection in deep learning has spawned an own line of research and method development. Among others, changes in architecture DeVries and Taylor [2018], loss function Sensoy et al. [2018], van Amersfoort et al. [2020] and the incorporation of data serving as OoD proxy Hendrycks et al. [2019] have been considered in the literature. Generative adversarial networks (GANs) have been used to replace that proxy by artificially generated data examples. In Lee et al. [2018a], examples of OoD data are created such that they shield the in-distribution regime from the OoD regime. Note that this often requires pre-training of the generator. E.g. in the aforementioned work, the authors constructed OoD data in their 2D example to pretrain the generator. While showing promising results, such GAN-based approaches mostly predict a single score for OoD detection and do not yield a principled approach to uncertainty quantification distinguishing in-distribution uncertainty between classes and out-of-distribution uncertainty.

In this work, we propose to use GANs to, instead of shielding all classes at once, shield each class separately from the out-of-class (OoC) regime (also cf. Figure 1). Instead of maximizing an uncertainty measure, like softmax entropy, we combine this with a one-vs-all classifier in the final DNN layer. This is learned jointly with a class-conditional generator for out-of-class data in an adversarial framework. The resulting classifiers are used to model (class conditional) likelihoods. Via Bayes rule we define posterior class probabilities in a principled way. Our work thus makes the following novel contributions:

1. We introduce a GAN-based model yielding a classifier with complete uncertainty quantification.
2. Our model allows to distinguish uncertainty between classes (in large sample limit, if properly learned, approaching aleatoric uncertainty) from OoD uncertainty (approaching epistemic uncertainty).
3. By a conditional GAN trained with a Wasserstein-based loss function, we achieve class shielding in low dimensions without any pre-training of the generator.
4. In higher dimensions, we use a class conditional autoencoder and train the GAN on the latent space. This is coherent with the conditional GAN, allows us to use less complex generators and critics and reduces the influence of adversarial directions.
5. We improve over the OoD detection and FP detec-

tion performance of state-of-the-art GAN-training based classifiers.

We present in-depth numerical experiments with our method on MNIST and CIFAR10, accompanied with various OoD datasets. We outperform other approaches, also GAN-based ones, in terms of OoD detection and FP detection performance on CIFAR10. Also on MNIST we achieve superior OoD detection performance. Noteworthy, on the more challenging CIFAR10 dataset, we achieve significantly stronger model accuracy compared to other approaches based on the same network architecture.

2 Related Work

The works by DeVries and Taylor [2018], Hendrycks and Gimpel [2017], Xia et al. [2015] can be considered as early baseline methods for the task of OoD detection. They are frequentist approaches relying on confidence scores gathered from model outputs. The problem is oftentimes the usage of the softmax activation function, which leads to overconfident predictions, in particular far away from training data, or to the decoupling of the confidence score from the original classification model during test time. Our proposed method does not make use of the softmax activation function and can produce unified uncertainty estimates during test time without the requirement of auxiliary confidence scores.

Many methods use perturbed training examples Lee et al. [2018b], Liang et al. [2018], Ren et al. [2019] or auxiliary outlier datasets Hendrycks et al. [2019], Kong and Ramanan [2021]. Lee et al. [2018b] use them for their confidence score based on class conditional Gaussian distributions, while Liang et al. [2018] and Ren et al. [2019] are utilizing them to increase the separability between in- and out-of-distribution examples. Hendrycks et al. [2019] use a hand picked auxiliary outlier dataset during model training and Kong and Ramanan [2021] use it for selecting a suitable GAN discriminator during training which then serves for OoD detection. The common problem with using perturbed examples is the sensitivity to hyperparameter selection which might render the resulting examples uninformative. Additionally, auxiliary outlier datasets cannot always be considered readily available and pose the problem of covering only a small proportion of the real world. In contrast, our method is able to produce OoC examples that are very close to the in-distribution but still distinguishable from it, thus we do not require explicit data perturbation or any auxiliary outlier datasets.

Bayesian approaches Blundell et al. [2015], Gal and Ghahramani [2015], Lakshminarayanan et al. [2017] provide a strong theoretical foundation for uncertainty quantification and OoD detection. Lakshminarayanan et al. [2017] propose deep ensembles that approximate

a distribution over models by averaging predictions of multiple independently trained models. Gal and Ghahramani [2015] are utilizing Monte-Carlo (MC) sampling with dropout applied to each layer. In Blundell et al. [2015] a variational learning algorithm for approximating the intractable posterior distribution over network weights has been proposed. While the theoretical foundation is strong, these methods often require changing the architecture, restricting the model space and/or increased computational cost. While making use of Bayes-rule, we are staying in a frequentist setting and are not dependent on sampling or ensemble techniques. This reduces computational cost and enables our model to produce high quality aleatoric and epistemic uncertainty estimates with a single forward pass. Also, our proposed framework does not change the network architecture, except for the output layer activation function, and thus makes it compatible with previously published techniques.

One-vs-All methods in the context of OoD detection have been recently studied by Franchi et al. [2020], Padhy et al. [2020], Saito and Saenko [2021]. In the work by Franchi et al. [2020] an ensemble of binary neural networks is trained to perform one-vs-all classification on the in-distribution data which are then weighted by a standard softmax classifier. Padhy et al. [2020] use a DNN with a single sigmoid binary output for every class and explore the possibility of training the one-vs-all network with a distance based loss function instead of the binary cross entropy. Domain adaptation is considered in Saito and Saenko [2021], where they utilize a one-vs-all classifier for a first OoD detection step before classifying into known classes with a second model. Their training objective is also accompanied by a hard negative mining on the in-distribution data. All these methods use the maximum predicted probability as a score for OoD detection and/or classification and do not aggregate the other probabilities into a single score like the method proposed by us. They also do not distinguish into different kinds of uncertainties as in our work. Lastly their training objectives are only based on in-distribution data. Generated OoD data as used in the present work is not considered.

More recently generative model based methods Lee et al. [2018a], Schlegl et al. [2017], Sricharan and Srivastava [2018], Sun et al. [2019], Vernekar et al. [2019b] have shown strong performance on the task of out-of-distribution detection by supplying classification models with synthesized out-of-distribution examples. Schlegl et al. [2017] utilize the latent space of a GAN by gradient based reconstruction of an input example. In the work by Lee et al. [2018a], a GAN architecture with an additional classification model is built. The classification model is trained to output a uniform distribution over classes on GAN examples close to the in-distribution. This approach is further improved by Sricharan and Srivastava [2018] who show improve-

ments on the task of out-of-distribution detection. The generalization to distant regions in the sample space and the quality of generated boundary examples is however questionable Vernekar et al. [2019b]. A similar approach using a normalizing flow and randomly sampled latent vectors is proposed by Grcic et al. [2021]. The high level idea of the architectures proposed in the previously mentioned works is similar to the one proposed by us. However, other works are not able to approximate the boundary of data distributions with multiple modes as shown by Vernekar et al. [2019b]. Due to the fact that our GAN is class conditional and trained on a low dimensional latent space, we are able to follow multiple distribution modes resulting from different classes. We improve the in-distribution shielding by using a low-dimensional regularizer and have an additional advantage in terms of computational cost as our cGAN model architecture can be chosen with considerably smaller size due to it being trained in the latent space. Furthermore, these methods do not yield separate uncertainty scores for FP and OoD examples.

Generating OoD data based on lower dimensional latent representations has been explored in Sensoy et al. [2020], Vernekar et al. [2019a]. Vernekar et al. [2019a] utilize a variational Autoencoder (vAE) to produce examples that are inside the encoded manifold (type I) as well as outside of it (type II). Sensoy et al. [2020] also use a vAE and train a GAN in the resulting latent space, assigning generated examples to the OoD domain in order to estimate a Dirichlet distribution on the class predictions. Utilizing a vAE has the advantage that one can make assumptions on the distribution of the latent space. The downside, however, is that vAE are harder to train due to a vanishing Kullback-Leibler-Divergence (KL-Divergence), which is commonly applied to keep the posterior close to the prior distribution Fu et al. [2019]. While the work of Sensoy et al. [2020] is the most similar to our method, we improve on several shortcomings. First of all we employ class conditional models to improve diversity and class shielding. Additionally, we do not rely on a vAE which makes our approach more stable. Finally, we are able to distinguish aleatoric and epistemic uncertainty while the method by Sensoy et al. [2020] is not. It assigns the same type of uncertainty to OoD and FP examples.

3 Method

In this section we introduce our one-vs-all classifier and the GAN architecture including its losses and regularizers.

3.1 One-vs-All Classification

We start by formulating our classification model as a one-vs-all classifier. Let $C(o|x, y)$ model the probability

that for a given class $y \in \mathcal{Y} = \{1, \dots, n\}$, an example with features $x \in \mathcal{X} = \mathbb{R}^d$ is OoC. Analogously, $C(i|x, y) = 1 - C(o|x, y)$ for a given class y models the probability of x being in-class. We can consider $C(i|x, y)$ as a likelihood proxy for $p(x|y)$ and predict class labels by applying Bayes-rule:

$$p(y|x) = \frac{p(x|y)p(y)}{\sum_{y'=1}^n p(x|y')p(y')} \approx \frac{C(i|x, y)\hat{p}(y)}{\sum_{y'=1}^n C(i|x, y')\hat{p}(y')}, \quad (1)$$

with $\hat{p}(y)$ being the estimated relative class frequency (see Appendix A for a theoretic argument on this choice of likelihood proxy). We denote the right hand side of Equation (1) by $\hat{p}(y|x)$. Using $\hat{p}(y|x)$, we estimate the probability of an example x being in-distribution by defining

$$C(i|x) = \sum_{y=1}^n C(i|x, y)\hat{p}(y|x) \stackrel{(1)}{=} \sum_{y=1}^n \frac{C(i|x, y)^2 \hat{p}(y)}{\sum_{y'=1}^n C(i|x, y')\hat{p}(y')}, \quad (2)$$

which yields a quantification of epistemic uncertainty via $C(o|x) = 1 - C(i|x)$. For aleatoric uncertainty estimation, we consider the Shannon entropy of the predicted class probabilities

$$H(x) = - \sum_{y=1}^n \hat{p}(y|x) \log(\hat{p}(y|x)). \quad (3)$$

To model $C(i|x, y)$, we use a DNN with $n \geq 2$ output neurons equipped with sigmoid activations. For each class output y , the data corresponding to class y serves as in-class data and all other data as OoC data. Hence, a basic variant of our training objective is given by a weighted empirical binary cross entropy

$$\min_C \frac{1}{|\mathcal{X}|} \sum_{(x,y)} -\log(C(i|x, y)) - \frac{1}{n-1} \sum_{y' \neq y} \frac{\hat{p}(y)}{\hat{p}(y')} \log(C(o|x, y')). \quad (4)$$

Therein, $\hat{p}(y)$ is estimated from the in-class training set and $\frac{\hat{p}(y)}{\hat{p}(y')}$ is weighting the OoC loss to counter potential class imbalance. Similarly $\frac{1}{n-1}$ weighs the OoC loss compared to the in-class loss.

In addition, we generate for each class OoC examples with a conditional GAN. A joint training of classifier and GAN is introduced in the upcoming Section 3.2.

For comparison, both model architectures, with and without MC-Dropout, are discussed in the numerical experiments. Note that this demonstrates the compatibility of our model with existing methods.

3.2 GAN Architecture

Similar to Lee et al. [2018a], we combine our classification model with a GAN and train them alternately.

The Wasserstein GAN with gradient penalty proposed by Gulrajani et al. [2017] serves a basis for our conditional GAN (cGAN). Additionally, we condition the generator as well as the critic on the class labels to generate class specific OoC examples. Inspired by Sensoy et al. [2020], Vernekar et al. [2019a] who utilized the latent space of a variational autoencoder (vAE), we also train our GAN model on the latent space of an autoencoder. Thus, we do not produce adversarial noise in our examples and can use less complex generators and critics. In contrast to those works, we use a conditional vanilla autoencoder (cAE) instead of the vAE as we observed a more stable training. Prior to the cGAN training, we train the cAE on in-distribution data and then freeze the weights during the cGAN and classifier training. The optimization objective of the cAE is given as pixel-wise binary cross-entropy

$$\min_A \frac{1}{|\mathcal{X}|} \sum_{(x,y)} -\frac{1}{N_x} \sum_{i=1}^{N_x} x_i \cdot \log(\hat{x}_i) + (1 - x_i) \cdot \log(1 - \hat{x}_i), \quad (5)$$

with $\hat{x}_i = A_{\text{dec}}(z, y)$ the decoded latent variable, $z = A_{\text{enc}}(x)$ being the encoded example, x_i the i -th pixel of example x and N_x the number of pixels belonging to x . Therein, the pixel values are assumed to be in the interval $[0, 1]$, while $0 \cdot \log(0) = 0$.

The cGAN is trained using the objective function

$$\min_G \max_D \frac{1}{|\mathcal{X}|} \sum_{(x,y)} D(z|y) - D(\tilde{z}|y) + \lambda_{gp} \cdot L_{gp}, \quad (6)$$

with D the conditional critic, $z = A_{\text{enc}}(x)$, $\tilde{z} = G(e, y)$ the latent embedding produced by the conditional generator, $e \sim U(0, 1)$ noise from a uniform distribution, y a class label and L_{gp} the gradient penalty from Gulrajani et al. [2017]. Integrating the classification objective into the cGAN objective, we alternate between

$$\min_G \max_D \overbrace{\frac{1}{|\mathcal{X}|} \sum_{(x,y)} D(z|y) - D(\tilde{z}|y) + \lambda_{gp} \cdot L_{gp}}^{L_{GD}} - \lambda_{cl} \cdot \log(C(o|\tilde{x}, y)) + \lambda_R L_R \quad (7)$$

and

$$\min_C \overbrace{\frac{1}{|\mathcal{X}|} \sum_{(x,y)} -\log(C(i|x, y))}^{L_C} - \frac{\lambda_{\text{real}}}{n-1} \left(\sum_{y' \neq y} \frac{\hat{p}(y)}{\hat{p}(y')} \log(C(o|x, y')) \right) - (1 - \lambda_{\text{real}}) \cdot \log(C(o|\tilde{x}, y)), \quad (8)$$

with $\lambda_{\text{real}} \in [0, 1]$ being an interpolation factor between real out-of-class examples and generated OoC examples

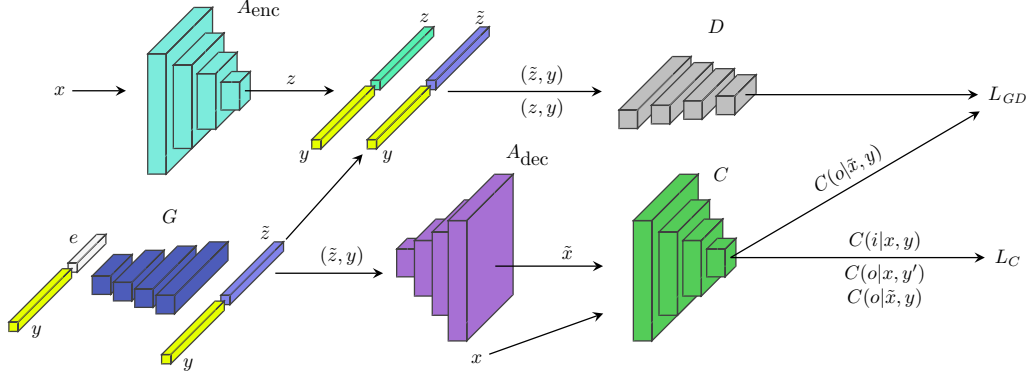


Figure 2: Overview of the proposed architecture. Before training the GAN objective together with the classifier, the cAE is pretrained on the in-distribution training dataset. After that the weights of A_{enc} and A_{dec} are frozen.

and L_R being an additional regularization loss for the generated latent codes with hyperparameter $\lambda_R \geq 0$, which we introduce in Section 3.3. The latent embeddings produced by the cGAN are decoded with the pretrained cAE, thus $\tilde{x} = A_{\text{dec}}(\tilde{z}, y) = A_{\text{dec}}(G(e, y), y)$. That is, the cGAN is trained on the latent space while the classification model is trained on the original feature space. Our entire GAN-architecture is visualized in Figure 2.

3.3 Low-Dimensional Regularizer

In low dimensional latent spaces we found it to be advantageous to apply an additional regularizer to the generated latent embeddings \tilde{z} to improve class shielding. Let (z, y) be the latent embedding of an example x with its corresponding class label y and $\mathcal{Z}(z, y) = \{\tilde{z} - z \mid \tilde{z} = G(e, y), e \sim U(0, 1)\}$ all generated latent codes with the same class label and normalized to origin z . We encourage the generator to produce latent codes that more uniformly shield the class y by maximizing the average angular distance between all $\tilde{z} \in \mathcal{Z}(z, y)$, which corresponds to minimizing

$$l_R(z, y) = \frac{2}{N_y^z \cdot (N_y^z - 1)} \cdot \sum_{\substack{\tilde{z}^i, \tilde{z}^j \in \mathcal{Z}(z, y) \\ i \neq j}} -\log \left(\arccos \left(\frac{\tilde{z}^i * \tilde{z}^j}{\|\tilde{z}^i\| \cdot \|\tilde{z}^j\|} \right) \cdot \frac{1}{\pi} \right), \quad (9)$$

with $*$ being the dot-product and $N_y^z = |\mathcal{Z}(z, y)|$. The logarithm introduces an exponential scaling for very small angular distances, encouraging a more evenly spread distribution of the generated latent codes. This loss is then averaged over all class labels and training data examples

$$L_R = \frac{1}{n} \sum_y \frac{1}{N_y} \sum_{(x, y)} l_R(A_{\text{enc}}(x), y), \quad (10)$$

with $N_y = |\{(x, y') \mid y' = y\}|$ the number of examples with class label y .

During our experiments we studied different regularizer losses such as manhattan/euclidean distance, infinity norm and standard cosine similarity. In experiments, we found that for our purpose Equation (10) performed best. We argue that this can be attributed to the independence of the latent space value range, which can have a large impact on the p -norm distance metrics and to the exponential scaling for very small angular distances.

4 Experiments

We compare our method with the following related works:

- **Maximum softmax** probability baseline by [Hendrycks and Gimpel \[2017\]](#)
- **Entropy** of the predictive class distribution
- **Bayes-by-Backprop** [Blundell et al. \[2015\]](#)
- **MC-Dropout** by [Gal and Ghahramani \[2015\]](#)
- **Deep-Ensembles** proposed by [Lakshminarayanan et al. \[2017\]](#)
- **Confident Classifier** proposed by [Lee et al. \[2018a\]](#)
- **GEN** by [Sensoy et al. \[2020\]](#)

While the first two methods are simple baselines, the next three ones are Bayesian ones and the final two methods are GAN-based (cf. Section 2). Following the publications [Hendrycks and Gimpel \[2017\]](#), [Ren et al. \[2019\]](#), [Sensoy et al. \[2020\]](#), [Vernekar et al. \[2019a\]](#), we consider two setups using the MNIST and CIFAR10 datasets as in-distribution, respectively. Similar to [Sensoy et al. \[2020\]](#), [Vernekar et al. \[2019a\]](#) and others, we split the datasets class-wise into two non-overlapping sets, i.e., MNIST 0-4 / 5-9 and CIFAR10 0-4 / 5-9. While the first half serves as in-distribution data, the second half constitutes OoD cases close to the training data and therefore difficult to detect. For the MNIST 0-4 dataset, we consider the MNIST 5-9,

EMNIST-Letters, Fashion-MNIST, Omniglot, SVHN and CIFAR10 datasets as OoD examples. For the CIFAR10 0-4 dataset, we use CIFAR10 5-9, LSUN, SVHN, Fashion-MNIST and MNIST as OoD examples. These selections yield compositions of training and OoD examples with strongly varying difficulty for state-of-the-art OoD detection. Besides that, we examine our method’s behavior on a 2D toy example with two overlapping Gaussians (having trivial covariance structure), see Figure 1. Additionally, we split the official training sets into 80% / 20% training / validation sets, where the latter are used for hyperparameter tuning and model selection.

Like related works, we utilize the LeNet-5 architecture on MNIST and a ResNet-18 on CIFAR10 as classification models. To ensure fair conditions, we re-implemented all aforementioned methods while following the authors recommendations for hyperparameters and their reference implementations. For methods involving more complex architectures, e.g. a GAN or a VAE as in Lee et al. [2018a], Sensoy et al. [2020], we used the proposed architectures for those components, while for the sake of comparability sticking to our choice of classifier models. All implementations are based on PyTorch Paszke et al. [2019] and will be published after the review phase. For each method, we selected the network checkpoint with maximal validation accuracy during training. For a more detailed overview of the used hyperparameters, we refer to Appendix C.

For evaluation we use the following well established metrics:

- **Classification accuracy** on the in-distribution datasets.
- **Area under the Receiver Operating Characteristic Curve (AUROC)**. We apply the AUROC to the binary classification tasks in-/out-of-distribution via Equation (2) and TP/FP (Success/Failure) via Equation (3).
- **Expected Calibration Error (ECE)** Naeini et al. [2015] applied to estimated class probabilities $\hat{p}(y|x)$ for in-distribution examples x , computed on 15 bins.
- **Area under the Precision Recall Curve (AUPR)** w.r.t. the binary in-/out-of-distribution decision in Equation (2). As the AUPR is sensitive to the choice of the positive class of that binary classification problem, we further distinguish between AUPR-In and AUPR-Out. For AUPR-in the in-distribution class is the positive one, while for AUPR-Out the out-of-distribution class is the positive one.
- **FPR @ 95% TPR** computes the **F**alse **P**ositive **R**ate (FPR) at the decision threshold on the OoD score from Equation (2) ensuring a **T**rue **P**ositive **R**ate (TPR) of 95%.



Figure 3: Generated OoD examples by our approach. a) MNIST examples for digit classes 0-4 (top to bottom). b) CIFAR10 examples for classes *airplane*, *automobile*, *bird*, *cat*, *deer* (top to bottom).

Before discussing our results on MNIST and CIFAR10, we briefly discuss our findings on the 2D example. As can be seen in Figure 1 the generated OoC examples are nicely shielding the respective in-distribution classes. OoC examples of one class can be in-distribution examples of other classes. This is an intended feature and to this end, the loss term for the synthesized OoC examples in Equation (8) is class conditional. This feature is supposed to make our likelihood proxy signal low density in the OoC regime. One can also observe that the estimated epistemic and aleatoric uncertainties are complementary, resulting in a high aleatoric uncertainty in the overlapping region of the Gaussians while also having a low epistemic uncertainty there. This is one of the main advantages that sets our approach apart from related methods. Results for a slightly more challenging 2D toy example on the two moons dataset are presented in Figure 4. We now demonstrate that this result generalizes to higher dimensional problems.

For MNIST and CIFAR10, Figure 3 shows the OoC examples produced at the end of the generator training. Due to using a conditional GAN and an AE, we are able to generate OoC examples (instead of only out-of-distribution as in related works) during test time. It can be seen that the resulting examples resemble a lot of semantic similarities with the original class while still being distinguishable from them.

All presented results are computed on the respective (official) test sets of the datasets. We also conducted an extensive parameter study on the validation sets, which is summarized in Appendix D. The conclusion of this parameter study is that the performance of our framework is in general stable w.r.t. the choice of the hyperparameters. Increasing λ_{reg} positively impacts the model performance up to a certain maximum. The best performance is obtained by choosing latent dimensions such that the cAE is able to compute reconstructions of good visual quality. Across all datasets, choosing

Method	In-Distribution			Out-of-Distribution			
	Accuracy \uparrow	AUROC S/F	ECE \downarrow	AUROC \uparrow	AUPR-In \uparrow	AUPR-Out \uparrow	FPR@95% TPR \downarrow
Ours	99.78 (0.09)	98.15 (1.78)	0.34 (0.18)	98.36 (0.10)	83.65 (1.00)	99.89 (0.01)	6.33 (0.80)
Ours with MC-Dropout	99.81 (0.01)	99.51 (0.11)	2.07 (0.19)	98.53 (0.27)	82.94 (2.39)	99.90 (0.02)	5.54 (0.84)
One-vs-All Baseline	99.84 (0.06)	99.84 (0.06)	0.22 (0.04)	97.13 (0.19)	66.51 (2.04)	99.81 (0.02)	9.52 (0.73)
Max. Softmax Entropy	99.87 (0.02)	99.68 (0.13)	0.11 (0.02)	97.07 (0.12)	69.00 (1.65)	99.81 (0.01)	9.71 (0.37)
Bayes-by-Backprop	99.87 (0.02)	99.66 (0.14)	0.11 (0.02)	97.13 (0.12)	68.76 (1.94)	99.81 (0.01)	9.65 (0.39)
Blundell et al. [2015]	99.67 (0.02)	99.50 (0.06)	0.78 (0.05)	95.46 (0.26)	67.09 (2.70)	99.60 (0.03)	17.33 (1.06)
MC-Dropout	99.91 (0.02)	99.62 (0.12)	0.83 (0.10)	97.69 (0.16)	72.82 (2.55)	99.86 (0.01)	8.28 (0.39)
Gal and Ghahramani [2015]	99.89 (0.03)	99.74 (0.08)	0.15 (0.01)	97.70 (0.03)	73.09 (0.62)	99.86 (0.00)	7.81 (0.21)
Deep-Ensembles	99.82 (0.02)	99.62 (0.15)	0.16 (0.01)	98.15 (0.13)	78.31 (2.01)	99.88 (0.01)	7.65 (0.46)
Lakshminarayanan et al. [2017]	99.70 (0.03)	98.13 (0.45)	1.98 (0.85)	97.78 (0.70)	69.77 (10.20)	99.86 (0.04)	8.98 (1.90)
Confident Classifier	99.79 (0.06)	98.93 (0.68)	0.82 (0.06)	99.90 (0.02)	98.66 (0.28)	99.99 (0.00)	0.43 (0.10)
Lee et al. [2018a]	99.78 (0.04)	99.26 (0.31)	0.30 (0.08)	99.87 (0.01)	98.01 (0.15)	99.99 (0.00)	0.64 (0.08)
GEN							
Sensory et al. [2020]							
Entropy Oracle							
One-vs-All Oracle							

Table 1: Results for MNIST (0-4) as in-distribution vs {MNIST (5-9), EMNIST-Letters, Omniglot, Fashion-MNIST, SVHN, CIFAR10} as out-of-distribution datasets

$\lambda_{\text{real}} \in [0.5, 0.6]$ achieves the best detection scores, also indicating a positive influence of the generated OoC examples on the model’s classification accuracy.

Tables 1 and 2 present the results of our numerical experiments. The scores in the columns of the section *In-Distribution* are solely computed on the respective in-distribution dataset, i.e., MNIST 0-4 and CIFAR10 0-4, respectively. The scores in the columns of the section *Out-of-Distribution* are displaying the OoD detection performance when presenting examples from the respective in-distribution dataset as well as from the entirety of all assigned OoD datasets. Note that we did not apply any balancing in the OoD datasets but included the respective test sets as (see Appendix C for the sizes of the test sets) is. As an upper bound on the OoD detection performance we also supply results for two oracle models, supplied with the real OoD training datasets they are evaluated on. One of them is trained with the standard softmax and binary-cross-entropy and the other one with our proposed loss function, cf. Equation (8)

We first discuss the in-distribution performance of our method. W.r.t. MNIST, the results given in the left section of Table 1 show that we are on par with state-of-the-art GAN-based approaches while still having a similar ECE, only being surpassed by MC-Dropout and the other baselines by a fairly small margin. However, considering the respective CIFAR10 results in the left section of Table 2, we clearly outperform state-of-the-art GAN-based methods as well as all other baseline methods by a large margin. Noteworthy, we achieve an accuracy of 90.58% which is 5 to 9 percent points (pp.) above the other classifiers and an AUROC S/F of 88.45% which is 3 to 6 pp. higher than for the other methods. This corresponds to a relative improvement of 35% in accuracy and 21% in AUROC S/F compared to the second best method. This shows that our model can utilize the GAN-generated OoC examples indeed to better localize aleatoric uncertainty, therefore better separating success and failure, and at the same time improving the classifier’s generalization. Furthermore,

we observe that the calibration errors yield mid-tier results compared to the other methods. This signals that, although we incorporate generated OoC examples impurifying the distribution of training data presented to the classifier, empirically there is no evidence that this harms the learned classifier, neither w.r.t. calibration, nor w.r.t. separation.

Considering the OoD results from the right-hand sections of Tables 1 and 2, the superiority of our method compared to the other ones is now consistent over both in-distribution datasets. On the MNIST dataset we are outperforming previously published works, especially considering the AUPR-In and FPR @ 95% TPR metrics, with a 25% and 28% relative improvement over the second best method, respectively. This is consistent with the results for CIFAR10 as in-distribution dataset where we achieve for both AUROC and AUPR-In a relative improvement of 20%–25% over the second best method.

Comparing our results with the ones of the oracles, two observations become apparent. Firstly, in some OoD experiments the GAN-generated OoC examples achieve results fairly close to the ones of the oracles while also in some of them there is still room for improvement left (in particular w.r.t. FPR@95%TPR). Secondly, GAN-generated OoC examples can help improve generalization (in terms of classification accuracy) while real OoD data might be too far away from the in-distribution data.

As a final experiment, we perform CIFAR10-based OoD and FP detection in the wild, i.e., we perform both tasks jointly while presenting in-distribution and OoD data in the same mix as in Table 2 to the classifier. To this end, we applied gradient boosting to the uncertainty scores provided by the respective methods to predict TP, FP and OoD. For the Bayesian approaches we considered the sample mean’s entropy and variance. The corresponding results are given in Table 3 in terms of class-wise accuracy. The main observations are that our method outperforms the other GAN-based methods and that our method including dropout achieves

Method	In-Distribution			Out-of-Distribution			
	Accuracy \uparrow	AUROC S/F \uparrow	ECE \downarrow	AUROC \uparrow	AUPR-In \uparrow	AUPR-Out \uparrow	FPR@ 95% TPR \downarrow
Ours	87.25 (0.25)	84.52 (0.46)	9.89 (0.27)	86.44 (0.65)	48.70 (1.17)	98.71 (0.08)	45.81 (2.88)
Ours with MC-Dropout	90.58 (0.25)	88.45 (0.19)	5.75 (0.60)	89.52 (0.23)	52.77 (0.40)	98.99 (0.03)	43.54 (1.50)
One-vs-All Baseline	82.83 (0.62)	81.69 (0.76)	8.27 (2.46)	72.10 (2.37)	31.40 (1.60)	95.99 (0.45)	88.60 (2.08)
Max. Softmax Hendrycks and Gimpel [2017]	82.42 (0.31)	83.29 (0.89)	11.34 (0.83)	72.52 (0.51)	30.52 (0.97)	96.10 (0.05)	87.68 (0.43)
Entropy	82.42 (0.31)	83.41 (0.88)	11.34 (0.83)	72.85 (0.49)	30.43 (0.87)	96.21 (0.06)	85.41 (0.89)
Bayes-by-Backprop Blundell et al. [2015]	84.05 (0.33)	85.22 (0.40)	9.17 (0.41)	74.23 (0.96)	29.91 (1.61)	96.48 (0.19)	83.97 (1.47)
MC-Dropout Gal and Ghahramani [2015]	85.08 (0.56)	83.91 (0.49)	9.90 (0.42)	77.56 (1.27)	38.75 (1.40)	96.85 (0.17)	82.35 (1.08)
Deep-Ensembles Lakshminarayanan et al. [2017]	85.43 (0.22)	85.29 (0.57)	3.10 (0.29)	74.24 (0.73)	32.81 (1.50)	96.43 (0.10)	85.07 (0.81)
Confident Classifier Lee et al. [2018a]	83.58 (0.11)	85.08 (0.18)	9.31 (0.80)	73.33 (0.53)	32.32 (1.09)	96.29 (0.11)	85.04 (1.09)
GEN Sensoy et al. [2020]	82.46 (0.35)	82.88 (0.49)	6.71 (1.81)	86.01 (1.60)	42.32 (2.81)	98.66 (0.17)	45.39 (3.26)
Entropy Oracle	83.41 (0.58)	80.73 (0.54)	7.53 (0.27)	95.44 (0.28)	68.51 (0.57)	99.57 (0.04)	17.27 (1.44)
One-vs-All Oracle	83.20 (0.49)	79.60 (0.29)	4.18 (0.48)	89.72 (0.68)	46.24 (1.86)	98.99 (0.08)	38.73 (2.20)

Table 2: Results for CIFAR10 (0-4) as in-distribution vs {CIFAR10 (5-9), LSUN, SVHN, Fashion-MNIST, MNIST} as out-of-distribution datasets

Method	Accuracy TP	Accuracy FP	Accuracy OoD
Ours	76.82 (1.25)	42.05 (3.82)	65.24 (0.67)
Ours + MC-Dropout	75.84 (0.33)	42.49 (3.80)	70.55 (1.62)
One-vs-All Baseline	66.28 (3.77)	33.48 (5.09)	56.96 (3.89)
Max. Softmax	64.98 (0.58)	33.58 (4.01)	48.77 (4.34)
Entropy	66.13 (1.07)	29.90 (5.67)	51.42 (4.62)
Bayes-by-Backprop	64.81 (0.93)	33.62 (4.31)	52.76 (4.31)
MC-Dropout	66.97 (1.88)	44.31 (2.14)	59.91 (2.10)
Deep-Ensembles	67.76 (0.56)	36.29 (1.78)	53.56 (1.01)
Confident Classifier	64.69 (1.47)	39.84 (3.85)	45.62 (3.47)
GEN	70.47 (0.94)	64.88 (1.52)	54.31 (2.52)
Entropy Oracle	71.36 (1.59)	61.40 (2.77)	82.35 (0.62)
One-vs-All Oracle	72.85 (1.33)	54.46 (1.43)	75.33 (1.33)

Table 3: Results obtained from aggregating predicted uncertainty estimates in a gradient boosting model which was then trained on a validation set.

the overall best performance. It can be observed that the Entropy Oracle performs very strong while using only a single uncertainty score. At a second glance, this is not surprising since an FP mostly involves the confusion of two classes while training the DNN to output maximal entropy on OoD examples is likely to result in the confusion of up to five classes, therefore yielding different entropy levels. We present a more detailed version of this experiment in Appendix E where we also take the estimated class probabilities $\hat{p}(y|x)$ into account.

An OoD-dataset-wise breakdown of the results in Tables 1 and 2 is provided in Appendix F. For MNIST, this breakdown reveals that our method performs particularly well in the difficult task of separating MNIST 0-4 and MNIST 5-9. On the other MNIST-related tasks we achieve mid-tier results, being slightly behind the other GAN-based methods. However, with regards to CIFAR10 we are consistently outperforming the other methods by large margins.

5 Conclusion

In this work, we introduced a GAN-based model yielding a one-vs-all classifier with complete uncertainty quantification. Our model distinguishes uncertainty

between classes (in large sample limit approaching aleatoric uncertainty) from OoD uncertainty (approaching epistemic uncertainty). We have demonstrated in numerical experiments that our model sets a new state-of-the-art w.r.t. OoD as well as FP detection. The generated OoC examples do not harm the training success in terms of calibration, but even improve it in terms of accuracy. We have seen that further incorporating MC dropout to account for model uncertainty can further improve the results.

Acknowledgment

M.R. acknowledges useful discussions with Hanno Gottschalk.

References

- Arsenii Ashukha, Alexander Lyzhov, Dmitry Molchanov, and Dmitry P. Vetrov. Pitfalls of in-domain uncertainty estimation and ensembling in deep learning. In *8th International Conference on Learning Representations, ICLR 2020, Addis Ababa, Ethiopia, April 26-30, 2020*. OpenReview.net, 2020.
- Charles Blundell, Julien Cornebise, Koray Kavukcuoglu, and Daan Wierstra. Weight uncertainty in neural networks. *CoRR*, abs/1505.05424, 2015.
- Terrance DeVries and Graham W. Taylor. Learning confidence for out-of-distribution detection in neural networks. *CoRR*, abs/1802.04865, 2018.
- Gianni Franchi, Andrei Bursuc, Emanuel Aldea, Séverine Dubuisson, and Isabelle Bloch. One versus all for deep neural network incertitude (OVNNI) quantification. *CoRR*, abs/2006.00954, 2020.
- Hao Fu, Chunyuan Li, Xiaodong Liu, Jianfeng Gao, Asli Celikyilmaz, and Lawrence Carin. Cyclical annealing schedule: A simple approach to mitigating

- KL vanishing. In Jill Burstein, Christy Doran, and Thamar Solorio, editors, *Proceedings of the 2019 Conference of the North American Chapter of the Association for Computational Linguistics: Human Language Technologies, NAACL-HLT 2019, Minneapolis, MN, USA, June 2-7, 2019, Volume 1 (Long and Short Papers)*, pages 240–250. Association for Computational Linguistics, 2019.
- Yarin Gal and Zoubin Ghahramani. Bayesian convolutional neural networks with bernoulli approximate variational inference. *CoRR*, abs/1506.02158, 2015.
- Jakob Gawlikowski, Cedrique Rovile Njieutcheu Tassi, Mohsin Ali, Jongseok Lee, Matthias Hünt, Jianxiang Feng, Anna M. Kruspe, Rudolph Triebel, Peter Jung, Ribana Roscher, Muhammad Shahzad, Wen Yang, Richard Bamler, and Xiao Xiang Zhu. A survey of uncertainty in deep neural networks. *CoRR*, abs/2107.03342, 2021.
- Ian J. Goodfellow, Jonathon Shlens, and Christian Szegedy. Explaining and harnessing adversarial examples. In Yoshua Bengio and Yann LeCun, editors, *3rd International Conference on Learning Representations, ICLR 2015, San Diego, CA, USA, May 7-9, 2015, Conference Track Proceedings*, 2015.
- Matej Grcic, Petra Bevandic, and Sinisa Segvic. Dense open-set recognition with synthetic outliers generated by real NVP. In Giovanni Maria Farinella, Petia Radeva, José Braz, and Kadi Bouatouch, editors, *Proceedings of the 16th International Joint Conference on Computer Vision, Imaging and Computer Graphics Theory and Applications, VISIGRAPP 2021, Volume 4: VISAPP, Online Streaming, February 8-10, 2021*, pages 133–143. SCITEPRESS, 2021.
- Ishaan Gulrajani, Faruk Ahmed, Martín Arjovsky, Vincent Dumoulin, and Aaron C. Courville. Improved training of wasserstein GANs. In Isabelle Guyon, Ulrike von Luxburg, Samy Bengio, Hanna M. Wallach, Rob Fergus, S. V. N. Vishwanathan, and Roman Garnett, editors, *Advances in Neural Information Processing Systems 30: Annual Conference on Neural Information Processing Systems 2017, December 4-9, 2017, Long Beach, CA, USA*, pages 5767–5777, 2017.
- Chuan Guo, Geoff Pleiss, Yu Sun, and Kilian Q. Weinberger. On calibration of modern neural networks. In Doina Precup and Yee Whye Teh, editors, *Proceedings of the 34th International Conference on Machine Learning, ICML 2017, Sydney, NSW, Australia, 6-11 August 2017*, volume 70 of *Proceedings of Machine Learning Research*, pages 1321–1330. PMLR, 2017.
- Kaiming He, Xiangyu Zhang, Shaoqing Ren, and Jian Sun. Deep residual learning for image recognition. In *2016 IEEE Conference on Computer Vision and Pattern Recognition, CVPR 2016, Las Vegas, NV, USA, June 27-30, 2016*, pages 770–778. IEEE Computer Society, 2016.
- Matthias Hein, Maksym Andriushchenko, and Julian Bitterwolf. Why ReLU networks yield high-confidence predictions far away from the training data and how to mitigate the problem. In *IEEE Conference on Computer Vision and Pattern Recognition, CVPR 2019, Long Beach, CA, USA, June 16-20, 2019*, pages 41–50. Computer Vision Foundation / IEEE, 2019.
- Dan Hendrycks and Kevin Gimpel. A baseline for detecting misclassified and out-of-distribution examples in neural networks. In *5th International Conference on Learning Representations, ICLR 2017, Toulon, France, April 24-26, 2017, Conference Track Proceedings*. OpenReview.net, 2017.
- Dan Hendrycks, Mantas Mazeika, and Thomas G. Dietterich. Deep anomaly detection with outlier exposure. In *7th International Conference on Learning Representations, ICLR 2019, New Orleans, LA, USA, May 6-9, 2019*. OpenReview.net, 2019.
- Eyke Hüllermeier and Willem Waegeman. Aleatoric and epistemic uncertainty in machine learning: an introduction to concepts and methods. *Mach. Learn.*, 110(3):457–506, 2021.
- Alex Kendall and Yarin Gal. What uncertainties do we need in bayesian deep learning for computer vision? In Isabelle Guyon, Ulrike von Luxburg, Samy Bengio, Hanna M. Wallach, Rob Fergus, S. V. N. Vishwanathan, and Roman Garnett, editors, *Advances in Neural Information Processing Systems 30: Annual Conference on Neural Information Processing Systems 2017, December 4-9, 2017, Long Beach, CA, USA*, pages 5574–5584, 2017.
- Diederik P. Kingma and Jimmy Ba. Adam: A method for stochastic optimization. In Yoshua Bengio and Yann LeCun, editors, *3rd International Conference on Learning Representations, ICLR 2015, San Diego, CA, USA, May 7-9, 2015, Conference Track Proceedings*, 2015. URL <http://arxiv.org/abs/1412.6980>.
- Shu Kong and Deva Ramanan. OpenGAN: Open-set recognition via open data generation. *CoRR*, abs/2104.02939, 2021.
- Alex Krizhevsky, Ilya Sutskever, and Geoffrey E. Hinton. ImageNet classification with deep convolutional neural networks. In Peter L. Bartlett, Fernando C. N. Pereira, Christopher J. C. Burges, Léon Bottou, and Kilian Q. Weinberger, editors, *Advances in Neural Information Processing Systems 25: 26th Annual*

- Conference on Neural Information Processing Systems 2012. Proceedings of a meeting held December 3-6, 2012, Lake Tahoe, Nevada, United States*, pages 1106–1114, 2012.
- Balaji Lakshminarayanan, Alexander Pritzel, and Charles Blundell. Simple and scalable predictive uncertainty estimation using deep ensembles. In Isabelle Guyon, Ulrike von Luxburg, Samy Bengio, Hanna M. Wallach, Rob Fergus, S. V. N. Vishwanathan, and Roman Garnett, editors, *Advances in Neural Information Processing Systems 30: Annual Conference on Neural Information Processing Systems 2017, December 4-9, 2017, Long Beach, CA, USA*, pages 6402–6413, 2017.
- Kimin Lee, Honglak Lee, Kibok Lee, and Jinwoo Shin. Training confidence-calibrated classifiers for detecting out-of-distribution samples. In *6th International Conference on Learning Representations, ICLR 2018, Vancouver, BC, Canada, April 30 - May 3, 2018, Conference Track Proceedings*. OpenReview.net, 2018a.
- Kimin Lee, Kibok Lee, Honglak Lee, and Jinwoo Shin. A simple unified framework for detecting out-of-distribution samples and adversarial attacks. In Samy Bengio, Hanna M. Wallach, Hugo Larochelle, Kristen Grauman, Nicolò Cesa-Bianchi, and Roman Garnett, editors, *Advances in Neural Information Processing Systems 31: Annual Conference on Neural Information Processing Systems 2018, NeurIPS 2018, December 3-8, 2018, Montréal, Canada*, pages 7167–7177, 2018b.
- Shiyu Liang, Yixuan Li, and R. Srikant. Enhancing the reliability of out-of-distribution image detection in neural networks. In *6th International Conference on Learning Representations, ICLR 2018, Vancouver, BC, Canada, April 30 - May 3, 2018, Conference Track Proceedings*. OpenReview.net, 2018.
- Martin Mundt, Iuliia Pliushch, Sagnik Majumder, and Visvanathan Ramesh. Open set recognition through deep neural network uncertainty: Does out-of-distribution detection require generative classifiers? In *2019 IEEE/CVF International Conference on Computer Vision Workshops, ICCV Workshops 2019, Seoul, Korea (South), October 27-28, 2019*, pages 753–757. IEEE, 2019.
- Mahdi Pakdaman Naeni, Gregory F. Cooper, and Milos Hauskrecht. Obtaining well calibrated probabilities using bayesian binning. In Blai Bonet and Sven Koenig, editors, *Proceedings of the Twenty-Ninth AAAI Conference on Artificial Intelligence, January 25-30, 2015, Austin, Texas, USA*, pages 2901–2907. AAAI Press, 2015.
- Shreyas Padhy, Zachary Nado, Jie Ren, Jeremiah Z. Liu, Jasper Snoek, and Balaji Lakshminarayanan. Revisiting one-vs-all classifiers for predictive uncertainty and out-of-distribution detection in neural networks. *CoRR*, abs/2007.05134, 2020.
- Adam Paszke, Sam Gross, Francisco Massa, Adam Lerer, James Bradbury, Gregory Chanan, Trevor Killeen, Zeming Lin, Natalia Gimelshein, Luca Antiga, Alban Desmaison, Andreas Kopf, Edward Yang, Zachary DeVito, Martin Raison, Alykhan Tejani, Sasank Chilamkurthy, Benoit Steiner, Lu Fang, Junjie Bai, and Soumith Chintala. Pytorch: An imperative style, high-performance deep learning library. In H. Wallach, H. Larochelle, A. Beygelzimer, F. d'Alché-Buc, E. Fox, and R. Garnett, editors, *Advances in Neural Information Processing Systems 32*, pages 8024–8035. Curran Associates, Inc., 2019.
- Jie Ren, Peter J. Liu, Emily Fertig, Jasper Snoek, Ryan Poplin, Mark A. DePristo, Joshua V. Dillon, and Balaji Lakshminarayanan. Likelihood ratios for out-of-distribution detection. In Hanna M. Wallach, Hugo Larochelle, Alina Beygelzimer, Florence d'Alché-Buc, Emily B. Fox, and Roman Garnett, editors, *Advances in Neural Information Processing Systems 32: Annual Conference on Neural Information Processing Systems 2019, NeurIPS 2019, December 8-14, 2019, Vancouver, BC, Canada*, pages 14680–14691, 2019.
- Kuniaki Saito and Kate Saenko. Ovanet: One-vs-all network for universal domain adaptation. *CoRR*, abs/2104.03344, 2021.
- Thomas Schlegl, Philipp Seeböck, Sebastian M. Waldstein, Ursula Schmidt-Erfurth, and Georg Langs. Unsupervised anomaly detection with generative adversarial networks to guide marker discovery. In Marc Niethammer, Martin Styner, Stephen R. Aylward, Hongtu Zhu, Ipek Oguz, Pew-Thian Yap, and Dinggang Shen, editors, *Information Processing in Medical Imaging - 25th International Conference, IPMI 2017, Boone, NC, USA, June 25-30, 2017, Proceedings*, volume 10265 of *Lecture Notes in Computer Science*, pages 146–157. Springer, 2017.
- Murat Sensoy, Lance M. Kaplan, and Melih Kandemir. Evidential deep learning to quantify classification uncertainty. In Samy Bengio, Hanna M. Wallach, Hugo Larochelle, Kristen Grauman, Nicolò Cesa-Bianchi, and Roman Garnett, editors, *Advances in Neural Information Processing Systems 31: Annual Conference on Neural Information Processing Systems 2018, NeurIPS 2018, December 3-8, 2018, Montréal, Canada*, pages 3183–3193, 2018.
- Murat Sensoy, Lance M. Kaplan, Federico Cerutti, and Maryam Saleki. Uncertainty-aware deep classifiers using generative models. In *The Thirty-Fourth AAAI Conference on Artificial Intelligence, AAAI*

- 2020, *The Thirty-Second Innovative Applications of Artificial Intelligence Conference, IAAI 2020, The Tenth AAAI Symposium on Educational Advances in Artificial Intelligence, EAAI 2020, New York, NY, USA, February 7-12, 2020*, pages 5620–5627. AAAI Press, 2020.
- Shai Shalev-Shwartz and Shai Ben-David. *Understanding Machine Learning - From Theory to Algorithms*. Cambridge University Press, 2014. ISBN 978-1-10-705713-5.
- Karen Simonyan and Andrew Zisserman. Very deep convolutional networks for large-scale image recognition. In Yoshua Bengio and Yann LeCun, editors, *3rd International Conference on Learning Representations, ICLR 2015, San Diego, CA, USA, May 7-9, 2015, Conference Track Proceedings*, 2015.
- Jasper Snoek, Yaniv Ovadia, Emily Fertig, Balaji Lakshminarayanan, Sebastian Nowozin, D. Sculley, Joshua V. Dillon, Jie Ren, and Zachary Nado. Can you trust your model’s uncertainty? evaluating predictive uncertainty under dataset shift. In Hanna M. Wallach, Hugo Larochelle, Alina Beygelzimer, Florence d’Alché-Buc, Emily B. Fox, and Roman Garnett, editors, *Advances in Neural Information Processing Systems 32: Annual Conference on Neural Information Processing Systems 2019, NeurIPS 2019, December 8-14, 2019, Vancouver, BC, Canada*, pages 13969–13980, 2019.
- Kumar Sricharan and Ashok Srivastava. Building robust classifiers through generation of confident out of distribution examples. *CoRR*, abs/1812.00239, 2018.
- Nitish Srivastava, Geoffrey E. Hinton, Alex Krizhevsky, Ilya Sutskever, and Ruslan Salakhutdinov. Dropout: a simple way to prevent neural networks from overfitting. *J. Mach. Learn. Res.*, 15(1):1929–1958, 2014.
- Ke Sun, Zhanxing Zhu, and Zhouchen Lin. Enhancing the robustness of deep neural networks by boundary conditional GAN. *CoRR*, abs/1902.11029, 2019.
- Joost van Amersfoort, Lewis Smith, Yee Whye Teh, and Yarin Gal. Uncertainty estimation using a single deep deterministic neural network. In *Proceedings of the 37th International Conference on Machine Learning, ICML 2020, 13-18 July 2020, Virtual Event*, volume 119 of *Proceedings of Machine Learning Research*, pages 9690–9700. PMLR, 2020.
- Ramon van Handel. Probability in high dimensions. 2016. URL <https://web.math.princeton.edu/~rvan/APC550.pdf>.
- Sachin Vernekar, Ashish Gaurav, Vahdat Abdelzad, Taylor Denouden, Rick Salay, and Krzysztof Czarnecki. Out-of-distribution detection in classifiers via generation. *CoRR*, abs/1910.04241, 2019a.
- Sachin Vernekar, Ashish Gaurav, Taylor Denouden, Buu Phan, Vahdat Abdelzad, Rick Salay, and Krzysztof Czarnecki. Analysis of confident-classifiers for out-of-distribution detection. *CoRR*, abs/1904.12220, 2019b.
- Yan Xia, Xudong Cao, Fang Wen, Gang Hua, and Jian Sun. Learning discriminative reconstructions for unsupervised outlier removal. In *2015 IEEE International Conference on Computer Vision, ICCV 2015, Santiago, Chile, December 7-13, 2015*, pages 1511–1519. IEEE Computer Society, 2015.

A Theoretical Consideration of the One-vs-All Classifier

In the in-distribution regime, i.e., for $(x, y) \sim p$, it might be more convenient to view our one-vs-all classifier $C(i|x, y)$ as an ensemble of binary classifiers

$$C_y(y'|x) \quad \text{with} \quad y' \in \{y, \neg y\} \quad \forall y \in \{1, \dots, n\}. \quad (11)$$

Therein, $\neg y$ denotes “not y ”, meaning any other class than y , and $p(\neg y|x) = \sum_{y' \neq y} p(y'|x)$. Each classifier C_y corresponding to class y learns to indicate whether it is more likely that a given $x \sim p_x$ (where p_x denotes the marginal distribution w.r.t. the input feature space) belongs to class y or not to class y . Under the assumption that C_y has the universal approximation property and that an empirical risk minimizer can be found (the former is true while the latter is NP-hard, however these are common assumptions in statistical learning theory [Shalev-Shwartz and Ben-David \[2014\]](#), [van Handel \[2016\]](#)), C_y in the large sample limit would converge to

$$C_y(y|x) \rightarrow p(y|x) = \frac{p(x|y)p(y)}{\sum_{y'=1}^n p(x|y')p(y')}, \quad (12)$$

if the training data (x, y) for the classifiers C_y was sampled i.i.d. according to $p(x, y)$ and we trained C_y with the binary cross entropy loss (Equation (4) without the weight factors $\frac{1}{n-1}$ and the class priors). However, since we balance the classes y in Equation (4), our classifier receives data sampled from $p(x|y)\tilde{p}(y)$ where $\tilde{p}(y) \equiv K$ is constant for all y . Hence, the classifier, if properly learned, converges to

$$C_y(y|x) \rightarrow \frac{p(x|y)K}{\sum_{y'=1}^n p(x|y')K} \propto p(x|y). \quad (13)$$

This justifies the selection of our one vs. all classifier as an approximation to the likelihood. However, this approximating property immediately disappears, once the generated examples from the GAN are also used as training data for the classifier. In Section 4, we demonstrate empirically that the GAN training does not reduce the overall classification accuracy. It also does neither worsen the capability of the classifier to separate TPs and FPs via aleatoric uncertainty, nor does it affect the calibration error, cf. Tables 1 and 2. In our numerical experiments on CIFAR10 in the main part of this work, we even find a significant improvement in terms of classification accuracy and separation of TPs and FPs compared to the one-vs-all baseline as well as the one-vs-all oracle. This reveals which positive effects GAN-examples can have not only on OoD detection but also on FP detection as well as classification accuracy.

B Two Moons - Toy Example

As a more challenging 2D example, we also present a result on the two moons dataset. In Figure 4, the results of an experiment with two separable classes is shown. In the top row of the figure, the training data is class-wise separable. In that case, we observe that the decision boundary also belongs to the OoD regime (top right panel), which is true as there is no in-distribution data present. Our model is able to learn this since the classes are shielded tightly enough such that the generated OoC examples are in part also located in the vicinity of the decision boundary. To better visualize the distribution of generated data, we depict estimated densities of the generated OoC data in the top right panel. For the aleatoric uncertainty in the top center panel, we observe that due to numerical issues, aleatoric uncertainty increases further away from the in-distribution data. However this can be accounted for by first considering epistemic uncertainty and then the aleatoric one. By this procedure, most of the examples close to the decision boundary would be correctly classified as OoD which is also correct since there is only a minor amount of aleatoric uncertainty involved in this example due to moderate sample size not being reflected by the data.

In the bottom row example, an experiment analogous to the top row but with a noisier version of the data is presented. The bottom left panel shows that the epistemic uncertainty on the decision boundary between the two classes clearly decreases in comparison to the top right panel. At the same time the bottom center panel shows that the gain in aleatoric uncertainty compared to the top center panel.

Note that for data points far away from the in-distribution regime, all $C(i|x, y)$ in take values close to zero. In practice this requires the inclusion of a small $\varepsilon > 0$ in the denominator to circumvent numerical problems in the logarithmic loss terms. In our experiments this also results in a high aleatoric uncertainty far away from the in-distribution as all estimated probabilities uniformly take the the lower bound’s value ε . However, a joint consideration of aleatoric and epistemic uncertainty disentangles this, since a high estimated probability of being

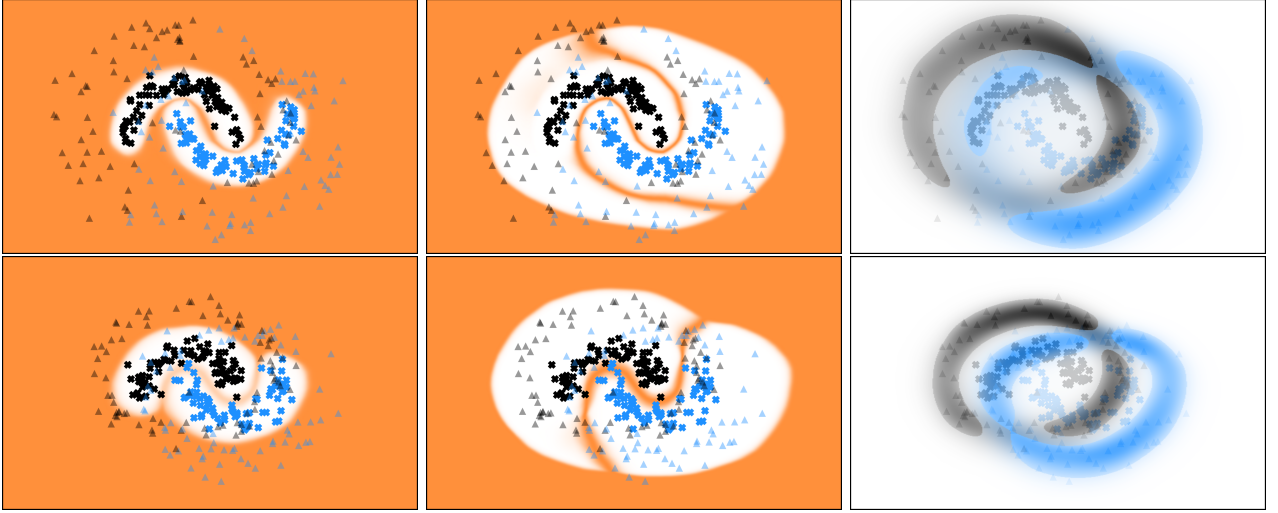


Figure 4: Two toy examples of the two moons dataset with different variance. From left to right: 1. OoD heatmap with orange indicating a high probability of being OoD and white for in-distribution; 2. Aleatoric uncertainty (entropy over Equation (1)) with orange indicating high and white low uncertainty; 3. Gaussian kernel density estimate of the GAN examples. Triangles indicate GAN OoC examples and crosses correspond to the in-distribution data. The data underlying the bottom row has higher variance than the one in underlying the top row.

OoD means that the estimate of aleatoric uncertainty can be neglected. This also becomes evident in the center panels where one can observe high aleatoric uncertainty $H(x)$ outside the in-distribution regime, which can however be masked out by the OoD probability $C(o|x)$.

C Hyperparameter Settings for Experiments

For the Bayes-by-Backprop implementation we use *spike-and-slap* priors in combination with diagonal Gaussian posterior distributions as described in Blundell et al. [2015]. MC-Dropout uses a 50% dropout probability on all weight layers. Both mentioned methods average their predictions over 50 forward passes. The deep-ensembles were built by averaging 5 networks. Implementations of Confident Classifier and GEN use the architectures and hyperparameters recommended by the authors and we followed their reference code where possible. Parameter studies showed that our method is mostly stable w.r.t. the hyperparameter selection. We used $\lambda_{gp} = 10$ as proposed in Gulrajani et al. [2017], $\lambda_{cl} = 2$ for MNIST and $\lambda_{cl} = 4$ for CIFAR10, $\lambda_{real} = 0.6$, $\lambda_R = 32$ for MNIST and $\lambda_R = 1$ for CIFAR10. The latent dimension for MNIST was set to 32 while using 128 dimensions for CIFAR10. We used batch stochastic gradient descent with the ADAM Kingma and Ba [2015] optimizer and a batch size of 256. The learning rate was initialized to 10^{-3} for the classification model and $2 \cdot 10^{-4}$ for the GAN while linearly decaying them to 10^{-5} over the course of all training iterations. Training on the MNIST dataset required 2000 generator iterations while taking 10000 iterations for the CIFAR10 dataset (one iteration is considered to be one batch). As recommended in Gulrajani et al. [2017], we use batch normalization only in the generator, while the critic as well as the classifier do not use any type of layer normalization. We also adopt the alternating training scheme from the just mentioned work. For each generator iteration the critic as well as classifier are performing 5 optimization steps on the same batch. We do apply some mild data augmentation by using random horizontal flipping where appropriate. The test set sizes used for computing the numerical results can be found in Table 4.

D Parameter Study

In order to examine the influence of hyperparameter selection onto our framework we conducted an extensive experimental study. We displayed all mentioned evaluation metrics from Section 4 while varying λ_{cl} , λ_{real} , λ_{reg} and the chosen latent dimension for the cAE and cGAN. For λ_{cl} in Equation (7), which controls the influence of the classifier predictions onto the generated OoC examples, Figure 5 shows clearly that for MNIST $\lambda_{cl} = 2$ and for CIFAR10 $\lambda_{cl} = 4$ are locally optimal values w.r.t. maximum performance. While larger λ_{cl} tend to

Dataset	Test-Set Size
MNIST 0-4	5 000
MNIST 5-9	5 000
CIFAR10 0-4	5 000
CIFAR10 5-9	5 000
EMNIST-Letters	20 800
Fashion-MNIST	10 000
SVHN	26 032
Omniglot	13 180
LSUN	10 000

Table 4: Test set sizes used for computing the numerical results.

increase the in-distribution accuracy slightly it greatly decreases all other evaluation metrics. A very interesting observation in Figure 6 about the influence of λ_{real} from Equation (8) is that both extremes ($\lambda_{\text{real}} \in \{0, 1\}$) are greatly decreasing the results. This shows clearly that the generated OoC examples have a positive effect on the OoD detection performance and in-distribution separability. In terms of the dimensionality of the latent space, Figure 7 shows that 32 and 128 dimensions are the optimal values for MNIST and CIFAR10, respectively. This is coherent with the visual quality of the examples decoded by the cAE, which does not improve much with higher dimensions. Analysing the influence of λ_{reg} in Figure 8 one can observe a positive effect on the results on the MNIST dataset by increasing the value of the parameter up to $\lambda_{\text{reg}} = 32$ where we reach a local maximum. It is also very apparent, that for $\lambda_{\text{reg}} = 0$ the results are comparatively bad, emphasizing the role of the low dimensional regularizer in our model. For CIFAR10 the effect is not as clear as for the MNIST dataset, but Figure 8 also shows a locally optimal setting of $\lambda_{\text{reg}} \in [1, 2]$. We believe that the higher latent dimension required for the CIFAR10 dataset and thus the curse of dimensionality is the main factor behind this finding.

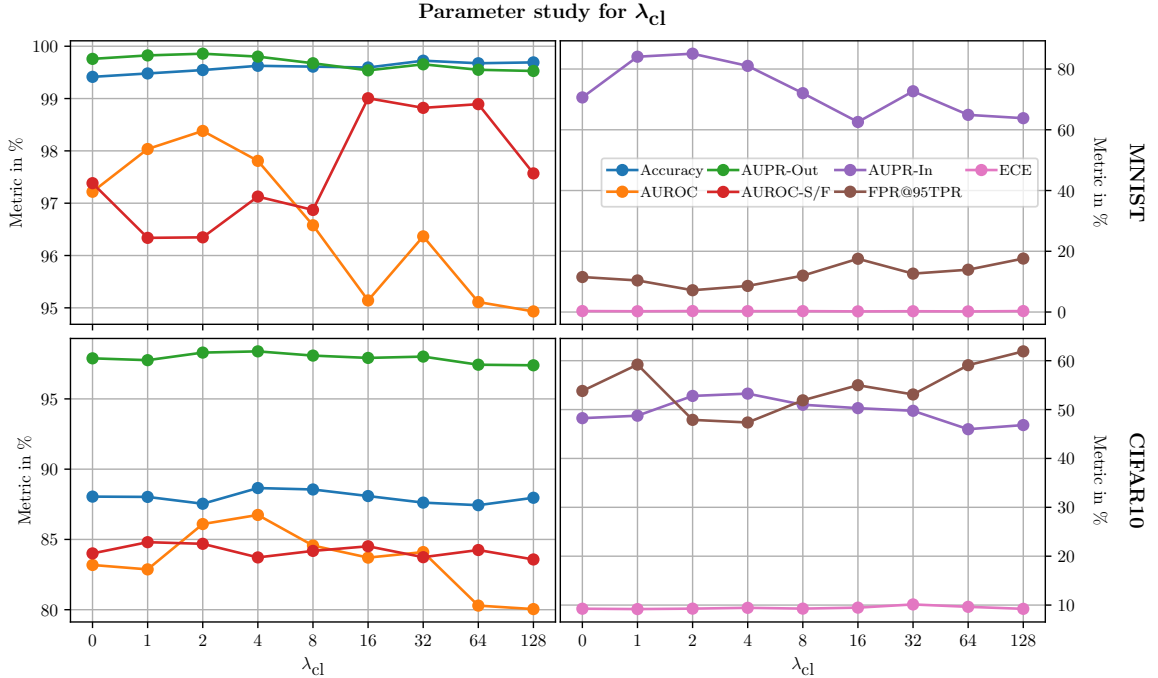


Figure 5: Parameter study over λ_{cl} in Equation (7). For MNIST hyperparameters were fixed at $\lambda_{\text{reg}} = 14$, $\lambda_{\text{real}} = 0.5$, latent dimension = 16 and for CIFAR10 at $\lambda_{\text{reg}} = 0$, $\lambda_{\text{real}} = 0.6$, latent dimension = 128. All seeds were also the same for all experiments. All metrics were computed on the validation sets of MNIST 0-4 / CIFAR10 0-4 as in-distribution datasets and the entirety of all assigned OoD datasets as defined in Section 4.

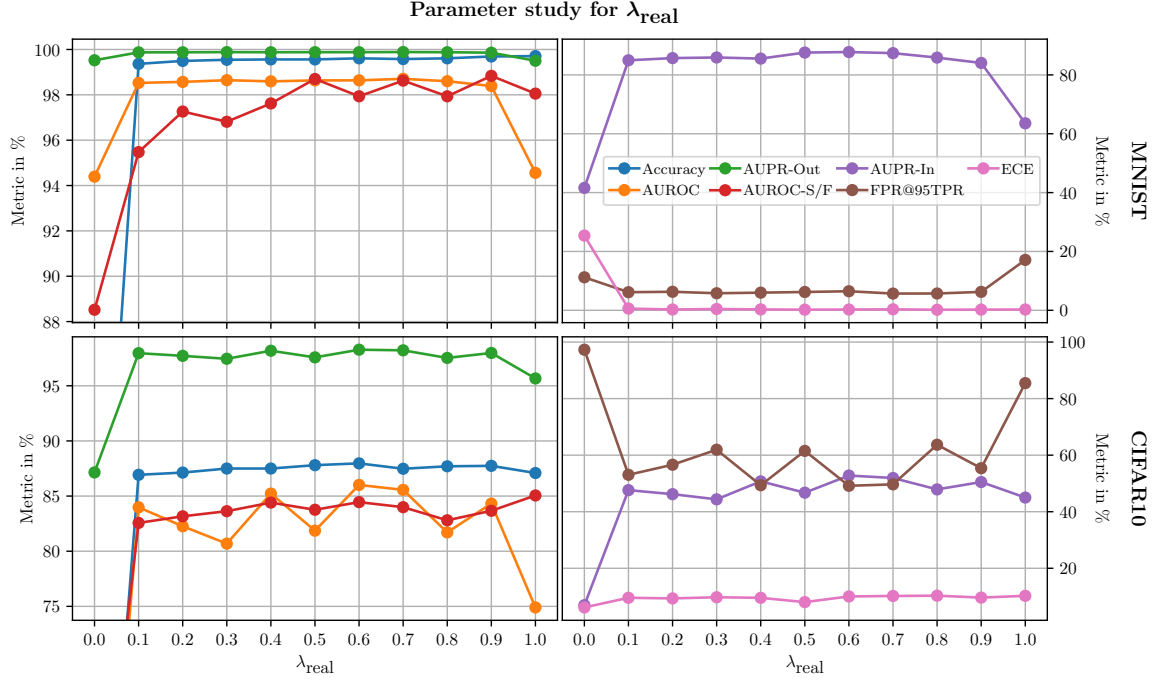


Figure 6: Parameter study over λ_{real} in Equation (8). For MNIST, hyperparameters were fixed at $\lambda_{\text{reg}} = 32$, $\lambda_{\text{cl}} = 1$, latent dimension = 16 and for CIFAR10 at $\lambda_{\text{reg}} = 0$, $\lambda_{\text{cl}} = 2$, latent dimension = 128. All seeds were also the same for all experiments. All metrics were computed on the validation sets of MNIST 0-4 / CIFAR10 0-4 as in-distribution datasets and the entirety of all assigned OoD datasets as defined in Section 4.

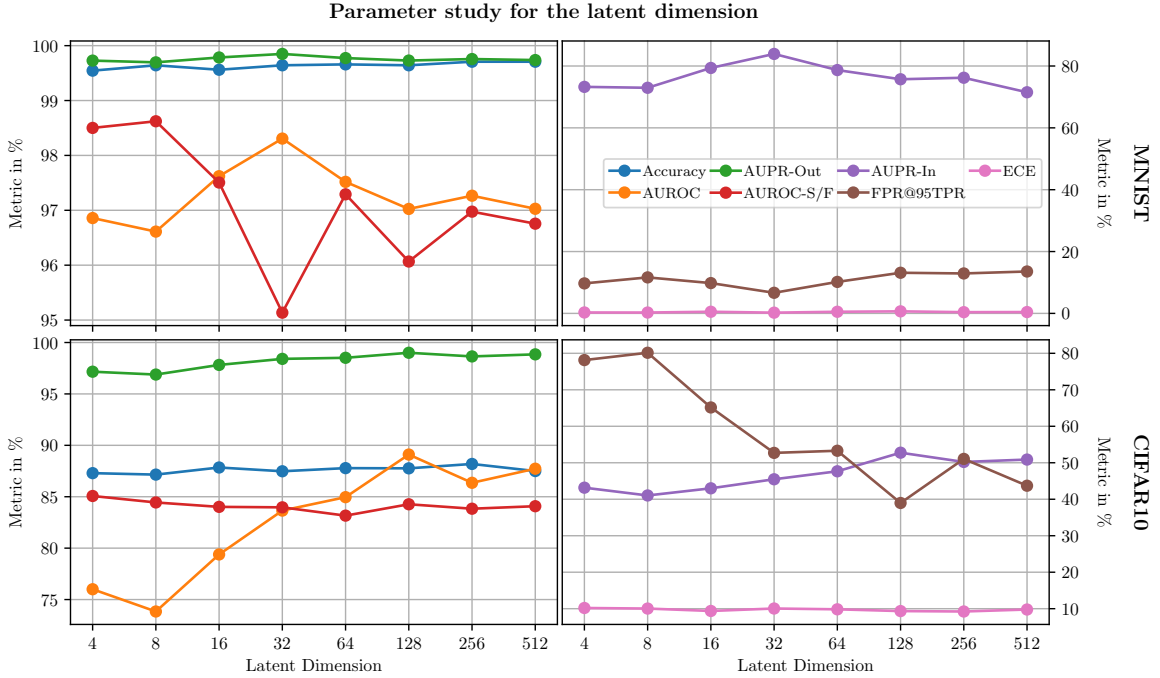


Figure 7: Parameter study over latent dimensions of z in Equation (7). For MNIST, hyperparameters were fixed at $\lambda_{\text{reg}} = 32$, $\lambda_{\text{cl}} = 1$, $\lambda_{\text{real}} = 0.5$ and for CIFAR10 at $\lambda_{\text{reg}} = 0$, $\lambda_{\text{cl}} = 4$, $\lambda_{\text{real}} = 0.6$. All seeds were also the same for all experiments. All metrics were computed on the validation sets of MNIST 0-4 / CIFAR10 0-4 as in-distribution datasets and the entirety of all assigned OoD datasets as defined in Section 4.

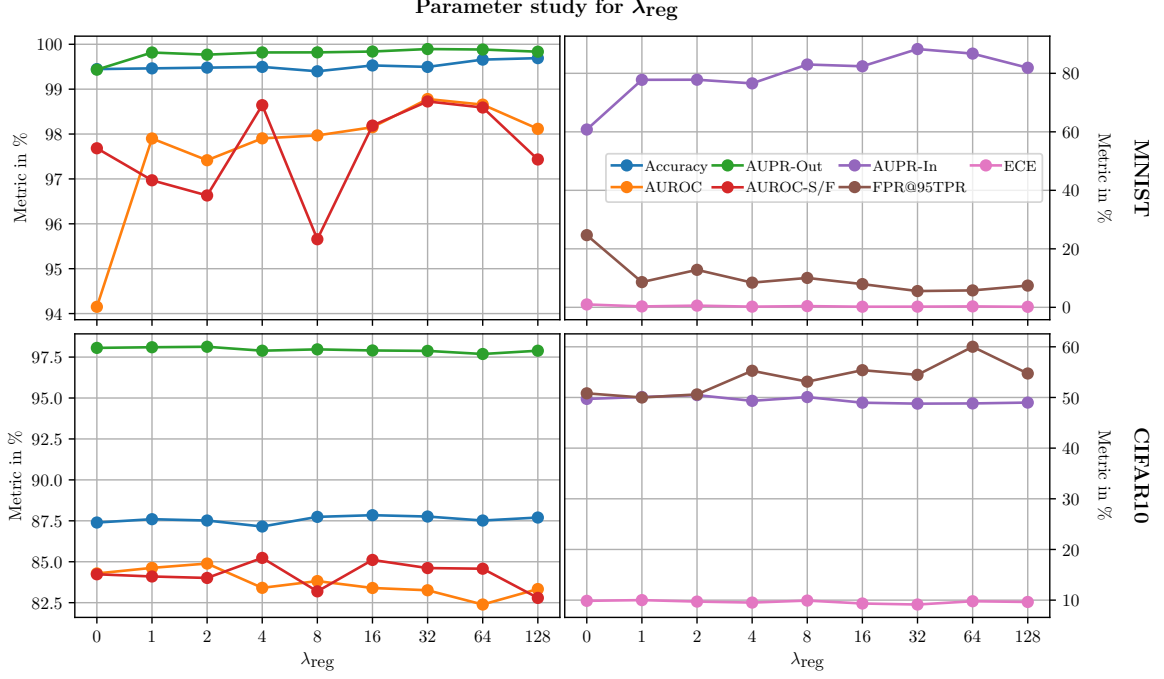


Figure 8: Parameter study over λ_{reg} in Equation (7). For MNIST, hyperparameters were fixed at $\lambda_{\text{cl}} = 1$, $\lambda_{\text{real}} = 0.5$, latent dimension = 16 and for CIFAR10 at $\lambda_{\text{cl}} = 4$, $\lambda_{\text{real}} = 0.6$, latent dimension = 128. All seeds were also the same for all experiments. All metrics were computed on the validation sets of MNIST 0-4 / CIFAR10 0-4 as in-distribution datasets and the entirety of all assigned OoD datasets as defined in Section 4.

E Joint Detection of OoD and FP

Method	Uncertainty Scores and Predicted Probabilities			Uncertainty Scores Only		
	Accuracy TP	Accuracy FP	Accuracy OoD	Accuracy TP	Accuracy FP	Accuracy OoD
Ours	78.71 (1.00)	38.15 (1.40)	75.00 (0.76)	76.82 (1.25)	42.05 (3.82)	65.24 (0.67)
Ours with MC-Dropout	79.50 (0.93)	48.26 (2.99)	82.25 (0.62)	75.84 (0.33)	42.49 (3.80)	70.55 (1.62)
One-vs-All Baseline	67.97 (1.78)	46.87 (1.89)	73.73 (1.94)	66.28 (3.77)	33.48 (5.09)	56.96 (3.89)
Max. Softmax Hendrycks and Gimpel [2017]	66.04 (0.33)	49.51 (1.69)	71.55 (1.48)	64.98 (0.58)	33.58 (4.01)	48.77 (4.34)
Entropy	66.98 (0.56)	48.47 (1.74)	72.36 (1.33)	66.13 (1.07)	29.90 (5.67)	51.42 (4.62)
Bayes-by-Backprop Blundell et al. [2015]	67.98 (0.88)	44.65 (2.05)	73.34 (0.99)	64.81 (0.93)	33.62 (4.31)	52.76 (4.31)
MC-Dropout Gal and Ghahramani [2015]	72.20 (0.41)	52.53 (1.29)	77.38 (0.49)	66.97 (1.88)	44.31 (2.14)	59.91 (2.10)
Deep-Ensembles Lakshminarayanan et al. [2017]	72.10 (0.33)	47.76 (0.90)	75.30 (0.41)	67.76 (0.56)	36.29 (1.78)	53.56 (1.01)
Confident Classifier Lee et al. [2018a]	68.15 (0.77)	50.64 (1.45)	72.23 (0.71)	64.69 (1.47)	39.84 (3.85)	45.62 (3.47)
GEN Sensoy et al. [2020]	69.86 (2.11)	49.13 (2.43)	76.04 (1.17)	70.47 (0.94)	64.88 (1.52)	54.31 (2.52)
Entropy Oracle	76.89 (0.32)	54.33 (2.05)	86.59 (0.37)	71.36 (1.59)	61.40 (2.77)	82.35 (0.62)
One-vs-All Oracle	74.90 (0.73)	54.36 (1.72)	80.13 (1.10)	72.85 (1.33)	54.46 (1.43)	75.33 (1.33)

Table 5: Results obtained from aggregating predicted uncertainty estimates in a gradient boosting model which was then trained on a validation set.

Table 5 presents an extended version of Table 3 where the latter constitutes the right-hand half of the former. While the right-hand half presents results for gradient boosting applied to the uncertainty scores of each method, aiming to predict TP, FP and OoD, the left half of the table shows analogous results while additionally using the estimated class probabilities $\hat{p}(y|x)$ as inputs for gradient boosting. We do so for the sake of accounting for other possible transformations of $\hat{p}(y|x)$ that are not explicitly constructed. In more detail, we use the following uncertainty scores:

- Ours: OoD uncertainty $C(o|x)$ and entropy $H(x)$ of the estimated class probabilities
- Ours with MC dropout: $C(o|x)$, $H(x)$ and the standard deviations of $\hat{p}(y|x)$ summed over all $y = 1, \dots, n$ under MC dropout for 50 forward passes.
- One-vs-All Baseline: Same as “Ours”.
- Max softmax: Maximum softmax probability.

Method	AUROC \uparrow	AUPR-In \uparrow	AUPR-Out \uparrow	FPR@ 95% TPR \downarrow	AUROC \uparrow	AUPR-In \uparrow	AUPR-Out \uparrow	FPR@ 95% TPR \downarrow
MNIST 0-4 vs. MNIST 5-9					MNIST 0-4 vs. EMNIST-Letters			
Ours	93.86 (0.87)	94.23 (1.28)	91.54 (0.92)	27.63 (4.39)	97.23 (0.32)	89.13 (1.46)	99.31 (0.08)	10.96 (1.20)
Ours + Dropout	95.61 (0.68)	96.31 (0.77)	93.67 (0.94)	23.18 (2.72)	96.56 (0.54)	86.11 (2.41)	99.14 (0.13)	12.70 (1.59)
One-vs-All Baseline	93.70 (1.01)	92.38 (1.42)	94.32 (0.90)	20.40 (3.60)	91.24 (0.35)	70.20 (1.51)	97.66 (0.11)	29.71 (1.50)
Max. Softmax	92.77 (0.55)	91.46 (1.05)	93.58 (0.26)	22.17 (1.04)	91.63 (0.28)	73.52 (1.02)	97.72 (0.07)	29.31 (0.88)
Entropy	92.80 (0.54)	91.20 (1.27)	93.63 (0.24)	22.11 (1.04)	91.68 (0.27)	73.51 (1.14)	97.73 (0.07)	29.23 (0.91)
Bayes-by-Backprop	93.73 (0.99)	92.74 (1.58)	93.83 (0.69)	22.17 (1.40)	90.59 (0.80)	71.60 (2.22)	97.34 (0.23)	34.28 (1.54)
MC-Dropout	94.32 (1.10)	93.05 (1.79)	95.19 (0.70)	17.27 (1.60)	92.80 (0.37)	76.85 (1.53)	98.09 (0.09)	26.72 (1.00)
Deep-Ensembles	94.20 (0.24)	92.82 (0.18)	95.00 (0.28)	16.89 (1.09)	93.08 (0.10)	77.32 (0.73)	98.16 (0.02)	24.65 (0.37)
Confident Classifier	95.33 (0.74)	95.43 (1.00)	94.95 (0.64)	19.74 (1.46)	94.60 (0.41)	81.71 (1.56)	98.53 (0.11)	22.28 (1.87)
GEN	88.91 (2.64)	86.09 (4.55)	88.15 (2.20)	40.49 (5.53)	99.27 (0.30)	97.05 (1.22)	99.82 (0.07)	3.61 (1.48)
Entropy Oracle	99.76 (0.04)	99.77 (0.03)	99.74 (0.04)	0.93 (0.12)	99.84 (0.04)	99.43 (0.12)	99.96 (0.01)	0.73 (0.21)
One-vs-All Oracle	99.53 (0.06)	99.52 (0.06)	99.54 (0.05)	1.84 (0.29)	99.74 (0.03)	98.98 (0.10)	99.94 (0.01)	1.46 (0.21)
MNIST 0-4 vs. Omniglot					MNIST 0-4 vs. Fashion-MNIST			
Ours	97.26 (0.53)	95.64 (0.98)	98.43 (0.29)	12.23 (4.35)	99.49 (0.14)	99.30 (0.19)	99.68 (0.09)	0.92 (0.66)
Ours + Dropout	98.44 (0.23)	96.98 (0.34)	99.23 (0.14)	5.65 (1.03)	99.63 (0.27)	99.49 (0.36)	99.76 (0.18)	0.70 (1.07)
One-vs-All Baseline	98.75 (0.12)	97.62 (0.23)	99.41 (0.06)	4.65 (0.82)	99.44 (0.11)	99.21 (0.14)	99.62 (0.10)	1.43 (0.51)
Max. Softmax	98.54 (0.06)	97.10 (0.24)	99.31 (0.02)	5.52 (0.50)	99.29 (0.23)	99.03 (0.36)	99.53 (0.15)	1.79 (1.34)
Entropy	98.59 (0.06)	97.15 (0.24)	99.35 (0.01)	5.36 (0.50)	99.35 (0.22)	99.06 (0.36)	99.59 (0.15)	1.74 (1.31)
Bayes-by-Backprop	96.82 (0.16)	95.22 (0.30)	97.46 (0.23)	14.86 (0.56)	97.93 (0.18)	97.64 (0.24)	98.26 (0.20)	8.02 (1.30)
MC-Dropout	98.96 (0.09)	97.56 (0.27)	99.58 (0.03)	3.85 (0.43)	99.69 (0.05)	99.52 (0.08)	99.83 (0.03)	0.75 (0.21)
Deep-Ensembles	98.93 (0.04)	97.77 (0.07)	99.52 (0.02)	3.76 (0.20)	99.59 (0.09)	99.38 (0.15)	99.76 (0.05)	1.01 (0.63)
Confident Classifier	98.35 (0.29)	96.22 (0.83)	99.29 (0.11)	6.78 (1.06)	99.95 (0.01)	99.91 (0.03)	99.97 (0.01)	0.06 (0.02)
GEN	91.03 (3.53)	78.34 (9.87)	94.92 (1.67)	36.96 (9.71)	99.92 (0.02)	99.84 (0.04)	99.96 (0.01)	0.23 (0.11)
Entropy Oracle	99.68 (0.09)	99.25 (0.21)	99.87 (0.04)	1.26 (0.35)	100.00 (0.00)	100.00 (0.00)	100.00 (0.00)	0.00 (0.00)
One-vs-All Oracle	99.71 (0.03)	99.28 (0.07)	99.89 (0.01)	1.13 (0.16)	100.00 (0.00)	100.00 (0.00)	100.00 (0.00)	0.00 (0.00)
MNIST 0-4 vs. SVHN					MNIST 0-4 vs. CIFAR10			
Ours	99.72 (0.14)	99.36 (0.28)	99.93 (0.04)	0.12 (0.08)	99.70 (0.16)	99.61 (0.19)	99.81 (0.11)	0.15 (0.11)
Ours + Dropout	99.78 (0.25)	99.42 (0.56)	99.94 (0.08)	0.35 (0.44)	99.82 (0.21)	99.75 (0.28)	99.89 (0.14)	0.30 (0.51)
One-vs-All Baseline	99.80 (0.07)	99.36 (0.17)	99.94 (0.04)	0.33 (0.11)	99.61 (0.16)	99.44 (0.21)	99.73 (0.14)	0.65 (0.39)
Max. Softmax	99.68 (0.12)	99.14 (0.24)	99.92 (0.04)	0.39 (0.12)	99.54 (0.13)	99.39 (0.17)	99.69 (0.10)	0.59 (0.30)
Entropy	99.75 (0.11)	99.22 (0.23)	99.94 (0.03)	0.37 (0.11)	99.61 (0.13)	99.45 (0.17)	99.76 (0.09)	0.56 (0.29)
Bayes-by-Backprop	97.20 (0.32)	95.75 (0.34)	98.77 (0.24)	11.46 (3.55)	97.52 (0.40)	97.48 (0.35)	97.11 (0.73)	7.44 (2.13)
MC-Dropout	99.94 (0.01)	99.75 (0.05)	99.99 (0.00)	0.15 (0.03)	99.92 (0.03)	99.87 (0.05)	99.96 (0.02)	0.09 (0.05)
Deep-Ensembles	99.89 (0.01)	99.55 (0.05)	99.98 (0.00)	0.25 (0.06)	99.82 (0.05)	99.73 (0.07)	99.90 (0.03)	0.20 (0.09)
Confident Classifier	100.00 (0.00)	100.00 (0.00)	100.00 (0.00)	0.00 (0.00)	100.00 (0.00)	100.00 (0.00)	100.00 (0.00)	0.00 (0.00)
GEN	100.00 (0.00)	100.00 (0.00)	100.00 (0.00)	0.00 (0.00)	100.00 (0.00)	100.00 (0.01)	100.00 (0.00)	0.01 (0.01)
Entropy Oracle	100.00 (0.00)	100.00 (0.00)	100.00 (0.00)	0.00 (0.00)	100.00 (0.00)	100.00 (0.00)	100.00 (0.00)	0.00 (0.00)
One-vs-All Oracle	100.00 (0.00)	100.00 (0.00)	100.00 (0.00)	0.00 (0.00)	100.00 (0.00)	100.00 (0.00)	100.00 (0.00)	0.00 (0.00)

Table 6: An OoD-dataset-wise breakdown of the results given in Table 1.

- Entropy: Entropy over estimated class probabilities.
- Bayes-by-Backprop: For $= 50$ samples from the posterior we compute $a = \frac{1}{K} \sum_1^K H(\hat{p}(y|x))$ (aleatoric uncertainty) and $b = H(\frac{1}{K} \sum_1^K \hat{p}(y|x)) - a$ (epistemic uncertainty) as in Kendall and Gal [2017].
- MC-Dropout: Entropy of estimated class probabilities averaged over 50 forward passes, standard deviation of the class probabilities summed over all $y = 1, \dots, n$.
- Deep-Ensembles: Entropy of estimated class probabilities averaged over 5 ensemble members, standard deviation of the class probabilities summed over all $y = 1, \dots, n$.
- Confident Classifier: Entropy over estimated class probabilities.
- GEN: Entropy over estimated class probabilities resulting of the estimated evidence of the Dirichlet distribution.

Also in the left part as well as the right part of the table, our method including dropout is fairly close the best oracle, which is the entropy oracle. The good performance of the entropy oracle can be explained by the fact that FPs typically only include the confusion of 2 classes while training on all OoD data for high entropy enforces the confusion among 5 classes, thus resulting in a higher entropy level. Apart from the oracle, in both studies including and excluding the estimated class probabilities $\hat{p}(y|x)$, our method including MC-dropout outperforms all other methods. However, reviewing the result in an absolute sense, there still remains plenty of room for improvement.

F Detailed Results on Individual OoD Datasets

In Section 4 we have presented results on the in-distribution datasets MNIST 0-4 and CIFAR10 0-4 versus the entirety of all respective OoD datasets (cf. Section 4). To give more detailed insights, this appendix section contains comparisons of the respective in-distribution dataset and each of the single corresponding OoD datasets.

Method	AUROC \uparrow	AUPR-In \uparrow	AUPR-Out \uparrow	FPR@ 95% TPR \downarrow	AUROC \uparrow	AUPR-In \uparrow	AUPR-Out \uparrow	FPR@ 95% TPR \downarrow
CIFAR10 0-4 vs. CIFAR10 5-9					CIFAR10 0-4 vs. LSUN			
Ours	65.97 (0.26)	72.00 (0.38)	64.39 (0.38)	86.94 (1.11)	76.53 (0.50)	69.36 (0.60)	84.27 (0.40)	80.58 (1.23)
Ours + Dropout	70.82 (0.45)	71.58 (0.34)	68.10 (0.53)	84.22 (0.85)	82.89 (0.75)	76.14 (0.89)	88.29 (0.51)	71.38 (1.19)
One-vs-All Baseline	64.47 (0.55)	65.51 (0.69)	62.46 (0.27)	88.06 (0.43)	74.15 (0.90)	65.06 (0.86)	82.71 (0.76)	82.27 (1.42)
Max. Softmax	64.45 (0.55)	65.94 (0.80)	60.77 (0.55)	90.73 (0.33)	72.84 (0.59)	63.69 (0.93)	80.70 (0.45)	87.11 (0.56)
Entropy	64.64 (0.53)	65.82 (0.69)	61.36 (0.50)	89.50 (0.69)	73.33 (0.51)	63.95 (0.90)	81.62 (0.39)	83.58 (0.56)
Bayes-by-Backprop	66.78 (0.34)	67.16 (1.07)	63.22 (0.50)	88.50 (0.62)	75.31 (0.65)	66.79 (1.13)	82.75 (0.68)	82.64 (1.16)
MC-Dropout	63.52 (0.33)	64.11 (0.38)	60.82 (0.27)	90.01 (0.39)	77.04 (0.22)	70.27 (0.41)	83.75 (0.12)	81.53 (0.59)
Deep-Ensembles	66.85 (0.38)	67.64 (0.57)	64.07 (0.31)	87.59 (0.42)	78.03 (0.24)	69.56 (0.47)	85.49 (0.20)	77.07 (0.66)
Confident Classifier	65.58 (0.13)	66.94 (0.18)	62.60 (0.29)	88.46 (0.64)	75.25 (0.33)	67.26 (0.41)	82.97 (0.36)	81.66 (0.99)
GEN	65.56 (0.50)	66.67 (0.51)	61.90 (0.67)	89.09 (1.17)	75.82 (1.22)	67.74 (1.65)	82.66 (0.75)	83.19 (1.91)
Entropy Oracle	73.21 (0.52)	75.00 (0.41)	70.70 (0.73)	81.41 (0.88)	98.27 (0.09)	96.81 (0.14)	99.11 (0.06)	7.91 (0.45)
One-vs-All Oracle	68.41 (0.47)	67.43 (0.57)	67.41 (0.70)	83.42 (1.34)	94.57 (0.44)	88.67 (0.91)	97.38 (0.21)	21.34 (1.90)
CIFAR10 0-4 vs. SVHN					CIFAR10 0-4 vs. Fashion-MNIST			
Ours	98.46 (0.27)	91.83 (1.15)	99.71 (0.05)	5.99 (1.27)	78.69 (0.79)	72.30 (0.87)	84.98 (0.84)	81.12 (2.84)
Ours + Dropout	98.89 (0.11)	94.12 (0.62)	99.79 (0.02)	5.16 (0.41)	84.13 (1.39)	79.95 (1.56)	87.63 (1.36)	77.46 (4.96)
One-vs-All Baseline	70.03 (4.23)	45.56 (4.33)	89.70 (1.93)	91.74 (3.33)	72.91 (2.70)	66.55 (2.50)	79.92 (1.93)	89.22 (1.57)
Max. Softmax	70.96 (1.87)	44.63 (2.22)	90.72 (0.66)	88.76 (1.38)	73.90 (1.18)	67.14 (1.35)	80.38 (0.97)	88.48 (0.82)
Entropy	71.23 (1.94)	44.81 (2.17)	90.87 (0.72)	87.04 (2.22)	73.93 (1.26)	67.18 (1.38)	80.30 (1.11)	88.47 (1.71)
Bayes-by-Backprop	76.21 (0.58)	50.10 (1.76)	92.92 (0.24)	80.85 (1.42)	74.51 (1.34)	68.52 (1.75)	80.67 (1.13)	88.11 (1.87)
MC-Dropout	76.73 (2.77)	58.97 (4.10)	92.23 (0.86)	84.98 (1.87)	81.85 (0.75)	77.62 (0.79)	85.83 (0.62)	80.75 (1.85)
Deep-Ensembles	72.02 (1.11)	45.95 (2.24)	90.96 (0.30)	88.13 (0.61)	72.82 (1.20)	66.38 (2.02)	79.25 (0.63)	89.97 (0.84)
Confident Classifier	73.60 (0.61)	48.68 (1.08)	91.71 (0.23)	85.45 (1.08)	74.47 (0.52)	68.40 (0.77)	80.85 (0.35)	87.47 (0.60)
GEN	98.43 (0.42)	91.36 (1.82)	99.71 (0.08)	5.62 (1.68)	72.44 (3.94)	66.54 (4.86)	79.12 (2.47)	89.38 (2.57)
Entropy Oracle	96.85 (0.62)	88.28 (1.42)	99.29 (0.21)	14.26 (2.88)	97.89 (0.16)	96.65 (0.28)	98.71 (0.10)	9.50 (0.61)
One-vs-All Oracle	88.01 (1.29)	63.81 (2.90)	97.17 (0.33)	47.42 (3.74)	94.06 (0.48)	88.87 (0.95)	96.76 (0.35)	26.30 (2.46)
CIFAR10 0-4 vs. MNIST								
Ours	83.08 (3.81)	75.36 (4.10)	90.27 (2.80)	58.77 (13.87)				
Ours + Dropout	86.51 (1.25)	81.97 (1.67)	91.43 (0.96)	61.31 (5.83)				
One-vs-All Baseline	78.43 (1.38)	74.14 (3.08)	83.30 (1.10)	86.36 (2.50)				
Max. Softmax	78.89 (1.79)	74.29 (2.40)	84.41 (1.37)	83.07 (2.10)				
Entropy	79.59 (1.81)	74.66 (2.38)	85.33 (1.55)	77.57 (3.12)				
Bayes-by-Backprop	71.46 (4.50)	62.19 (6.23)	79.41 (3.14)	87.01 (3.35)				
MC-Dropout	82.98 (1.21)	79.05 (1.68)	87.44 (0.83)	73.99 (1.97)				
Deep-Ensembles	81.33 (1.54)	76.97 (1.67)	85.98 (1.26)	78.85 (3.47)				
Confident Classifier	73.41 (2.43)	64.90 (4.16)	81.47 (1.62)	83.21 (2.58)				
GEN	87.63 (3.97)	80.69 (5.53)	93.31 (2.29)	45.16 (11.84)				
Entropy Oracle	97.59 (0.26)	97.10 (0.30)	97.82 (0.30)	10.16 (2.03)				
One-vs-All Oracle	95.60 (0.48)	93.33 (0.51)	96.94 (0.55)	23.59 (2.56)				

Table 7: An OoD-dataset-wise breakdown of the results given in Table 2.

The comparison by dataset for the MNIST 0-4 as in-distribution set in the OoD-dataset-wise breakdown given in Table 6 shows that we achieve mid-tier results compared to the other methods, except for when MNIST 5-9 is considered as the OoD dataset. In that challenging case, we achieve stronger results compared to the other methods. Examining the results of our OoD experiments with CIFAR10 0-4 being the in-distribution dataset in Table 7, it becomes apparent that we consistently outperform all other methods on each single OoD dataset. The performance gains are particularly pronounced when using the very similar datasets CIFAR10 5-9 and LSUN as OoD datasets. This consistency supports the finding that our method – especially in the case of OoD datasets very similar to the in-distribution dataset – shows the most improvement compared to other methods. This finding might be to some extent attributable to our tight class shielding.